Modelling, Measurement and Control A
Vol. 91, No. 2, June, 2018, pp. 48-53
Journal homepage: http://iieta.org/Journals/MMC/MMC_A

Operation in distributed power generation scheme with transition of control between stand-alone and grid connected modes

Rupa Mishra*, Tapas K. Saha

Department of Electrical Engineering, National Institute of Technology, Durgapur 713209, India

Corresponding Author Email: rupamishra123@gmail.com

https://doi.org/10.18280/mmc_a.910203

Received: 8 May 2018
Accepted: 27 June 2018

Keywords:
Induction generator, current control, voltage control, Pulse Width Modulation (PWM), Squirrel cage induction generator (SCIG), Total Harmonics Distortion (THD)

ABSTRACT

This paper presents flexible control strategy of a squirrel cage induction generator (SCIG) featuring transition between stand-alone and grid-connected systems. The consistent load voltage supply in both the modes is ensured with smooth transition of the controls of stand-alone and grid connected modes. In the proposed technique, dc bus voltage controller of the stand-alone system is maintaining the input power same as the demand by controlling the speed. On the other hand, the same dc bus voltage controller of the grid-connected system maintains the output power at same level as input power. The transient performances of different variables of the system, during this flexible control are found to be satisfactory and THD remains within 3% throughout the study. The flexible control for both the modes is presented for the first time in available literature. The model is helpful for interfacing into wind-energy system.

1. INTRODUCTION

Renewable energy sources such as wind, solar, and hydro are seen as a reliable choice to replace traditional energy sources i.e. oil or coal. Among the renewable energy sources, wind energy has the largest utilization in recent year. Now days, a doubly fed induction generator (DFIG) normally used in wind power generation systems due to its several advantages like variable speed operation, four-quadrant active and reactive power capability, maximized power capture, improved power quality [1]. But DFIG provides suitable choice at the site of at the site with low wind speed [2]. With the advent of power electronics, the demand of variable-speed squirrel cage induction generator (SCIG) with ac–dc–ac power conversion has become quite popular [3]. With the use of back to back converter, stand-alone mode of application with the proper control strategy has been already achieved [4].

The SCIG is operated to feed stand-alone load through a voltage source converter in [5], and control technique is done by simple vector control approach. Design and performance of grid-tied system, using double fed induction generator (DFIG) for wind application, was analyzed by [6-7]. The whole set up including voltage build up process and control algorithm for doubly operated induction generator (DOIG) fed to stand-alone load is discussed [8]. Design of Controller design by considering filter of DOIG based standalone variable speed constant frequency generator is provided in [9-11].

One of the peculiar characteristics of dispersed generation system is the capability to detach from the grid and endure to provide local loads during grid interruptions. Exchanging from a grid-tied mode to a stand-alone mode is known as islanding mode [12]. The algorithm matches the magnitude and phase of the inverter voltage and the grid voltage at the time of disconnecting or reconnecting to the grid to minimize any sudden voltage change across the load.

In a grid-tied mode, distributed generation units are controlled by active and reactive power control technique [13-14]. In a standalone mode, the distributed generation unit is controlled by voltage controller [15]. Thus latest challenges of power utilities are now adapt to operate in grid-tied and stand-alone modes, while ensuring a seamless transition between the two modes [16].

This study covers the flexible control of SCIG, fed by constant prime mover, to operate in grid-tied or stand-alone modes of operations and discusses the transition between these two modes in detail. During stand-alone mode of operation, the machine side converter is controlled to regulate the dc-link voltage by ensuring the input power to be same as output and uses three stages control. The load side converter is regulated to compensate the voltage drop of the filter. On the other hand the dc link voltage controller is implemented to ensure the output power to be same as input power by operating the load side converter for grid-tied system. Controller transitions during grid connection to stand-alone mode or vice-versa are studied and found satisfactory, first time in available literature.

2. SYSTEM CONFIGURATION

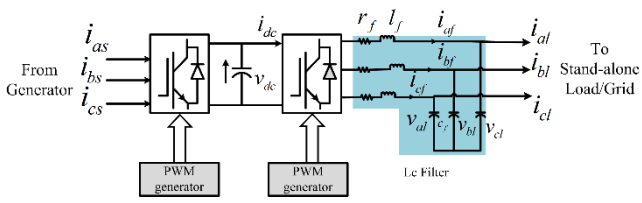

Figure 1. Schematic diagram of the SCIG fed to stand-alone and grid connected mode of operations

The proposed topology is shown in Fig.1 consists of a distributed generation connected to the stand-alone load or grid through back to back converter. A voltage source inverter

(VSI) is used to transfer the dc power to the ac load through LC filter during off grid (stand-alone) mode as shown in Fig.1.

3. CONTROL STRATEGY

3.1 Stand-alone mode

In case of stand-alone mode, the machine side converter control strategy is processed through dc link voltage and flux controller as shown in Fig. 2. The dc link voltage controller is developed to generate the speed command of the proposed topology as explained in (1) by maintain active power flow across it. The speed controller is accomplished through vector control and generating the torque command as shown in (2).

The reference value of the active power component i.e. q-axis component of machine current is generated from the speed controller as given in (3). The error of the q-axis component of machine current is passed through current controller to generate q-axis component of machine voltage as shown in (4). Similarly d-axis component of machine voltage is produced through current controller followed by flux controller as portrayed in (6).

$$\omega_r^* = \left[V_{dc}^* - V_{dc}\right]\left(k_{p1} + \frac{k_{i1}}{s}\right) \tag{1}$$

$$m_d^* = \left[\omega_r^* - \omega_r\right]\left(k_{p2} + \frac{k_{i2}}{s}\right) \tag{2}$$

where k_{p1}, k_{i1} and k_{p2}, k_{i2} are calculated from dc link voltage controller and speed controller respectively.

Torque equation can be written as

$$m_d = \frac{2}{3}\frac{p}{2} L_m i_{qs} \psi_r \tag{3}$$

where, rotor flux linkage $(\psi_r) = \frac{L_m i_{ds}}{1+s\tau}$

$$v_{qs}^* = \left(i_{qs}^* - i_{qs}\right)\left(k_p + \frac{k_i}{s}\right) \tag{4}$$

$$i_{ds}^* = \left|\psi_r^* - \psi_r\right|\left(k_{p1} + \frac{k_{i1}}{s}\right) \tag{5}$$

$$v_{ds}^* = \left(i_{ds}^* - i_{ds}\right)\left(k_p + \frac{k_i}{s}\right) \tag{6}$$

In this case, k_p, k_i value is estimated with the help of stator resistance and inductance. Here L_m denotes per phase magnetizing inductance. i_{qs}, i_{ds} are q,d-axis component of machine stator current respectively and ω_r is rotor speed of induction machine.

The load side converter works under voltage control mode to keep the output voltage constant, irrespective of the variation in load and input power. The d-axis load voltage reference is aligned with constant voltage vector in the synchronously rotating reference frame.

The filter voltage controller is generating the d-axis component of filter current reference as shown in Fig. 2. It tries to compensate the drop of the filter voltage. Using root locus method depicted in Fig. 3(a), proportionate controller value (k_{pd}) can be chosen as 1.29 to achieve damping ratio 1. From the bode plot, the bandwidth of voltage controller is taken as 2070 rad/s as shown in Fig. 3(b).

The q-axis component of the load voltage reference is kept to be zero. The voltage controller is generating the reference value of q-axis component of filter current. Then current controller generates the inverter d,q-axis voltages as shown in (7,8). This current controller (k_{pi}, k_{ii}) is designed with consideration of filter resistance and inductances. The bandwidth of the current loop is three times more than the voltage controller.

$$v_{di}^* = \left(i_{df}^* - i_{df}\right)\left(k_{pi} + \frac{k_{ii}}{s}\right) \tag{7}$$

$$v_{qi}^* = \left(i_{qf}^* - i_{qf}\right)\left(k_{pi} + \frac{k_{ii}}{s}\right) \tag{8}$$

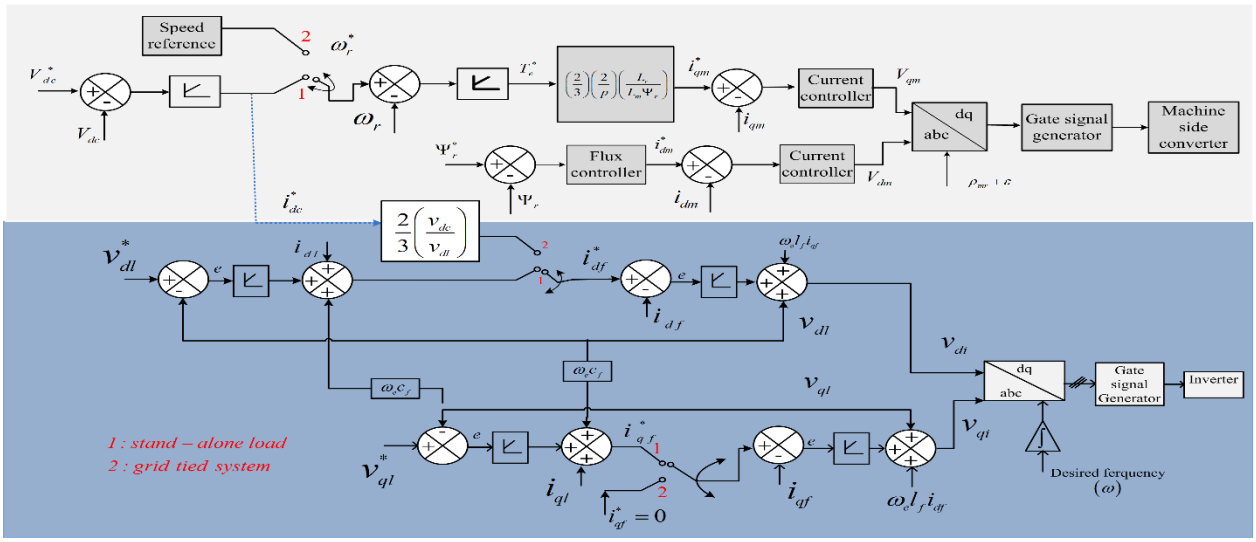

Figure 2. Control technique during stand-alone to grid transition and vice-versa

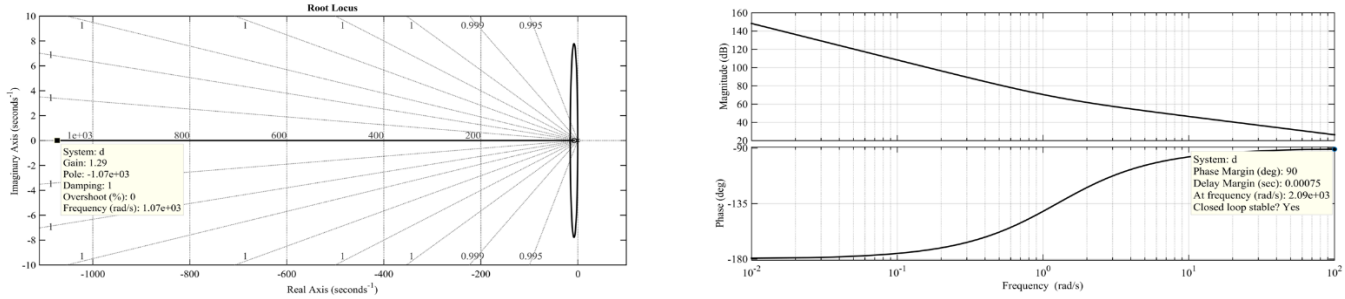

(a) (b)

Figure 3. Load voltage controller analysis (a) Time domain (b) Frequency domain

3.2 Grid connected mode

The dc link capacitor transfer extracted power from the machine to the utility with the availability of grid. The whole control strategy is developed by considering filter is portrayed in Fig. 2. The main objective of load side converter is to maintain the dc-link voltage constant and regulates the reactive power output to meet the grid requirements.

The dc link voltage controller is used to control the active power component of the grid $\left(i_d\right)$ as shown in Fig. 2. From this voltage controller dc link reference current is generated. By maintaining power balance across the dc link, the d-axis filter current is generated using (10) and (11). Following this the current passed through current controller to generate the q-axis voltage of the inverter as shown in (13). This voltage controller gain is calculated with the help of root locus. To achieve damping ratio 1 and zero percentage of overshoot, the gain of proportionate controller value $\left(k_p\right)$ is taken a as 0.0168 as portrayed in Fig. 4(a). By using bode plot as depicted in Fig. 4 (b), integrator time constant is estimated to achieve better dynamics. But reactive power component $\left(i_q\right)$ is kept at zero throughout the operation. A decoupling of the cross coupling term are considered to compensate the coupling effect.

$$i_{dc}^{*} = \left(v_{dc}^{*} - v_{dc}\right)\left(k_p + \frac{k_i}{s}\right) \tag{10}$$

$$v_{dc} i_{dc} = \frac{3}{2} v_{df}\, i_{df} \tag{11}$$

$$v_{di} = \left(i_{df}\, r_f\right) + l_f \frac{di_{df}}{dt} + v_{dg} - \omega_e l_f\, i_{qf} \tag{12}$$

$$v_{qi} = \left(i_{qf}\, r_f\right) + l_f \frac{di_{qf}}{dt} + v_{qg} + \omega_e l_f\, i_{df} \tag{13}$$

For machine side converter, d-axis component of machine voltage is generated in same way as the stand-alone mode of operation. Here the speed command is provided by user, unlike the earlier case, where it was been generated through dc-link voltage controller. The speed error passed through speed controller to generate reference torque. From the reference torque q-axis component of the machine current is generated as shown in Fig. 2. So maximum power point tracking is possible by this type of technique with suitable choice of speed command.

3.3 Transition from stand-alone mode to grid-tied mode

When grid is available, that instant inverter can't be fed directly to the utility grid because of high harmonics and transient in voltage. So for transition from stand-alone mode to grid connection, the load voltage magnitude, frequency and phase must be matched. In stand-alone mode dq to abc conversion is done by fixed phase angle which is different from grid angle. The transition strategy is incorporated by controller transition are as shown in Fig. 2.

4. SYSTEM DESCRIPTION

The power topology consist of two level VSI each having six IGBTs (900 V, 25 A), 1 hp, 750 rpm, 220 V, 7 A, 50 Hz SCIG fed to stand-alone and grid-tied system. Here dc link voltage is kept at 400 V. The load side filter, as shown in Fig. 1, is having parameters as: inductor kept at 8 mH, resistance is 0.1 Ω and capacitor value is 8.0938 μF. Filter resonant frequency is maintained at 625 Hz.

5. RESULTS AND DISCUSSION

During transition from standalone to grid connected mode at 2.5 sec and vice-versa at 8 sec, the transient performances of the machine and load variables are portrayed below. The dc link voltage is controlling machine power during stand-alone mode. But it delivers extracted power from the generator to the load, by generating d-axis component of the filter current during grid connected mode. So there is no such alteration in transient of load voltage during switching of modes. The Fig. 5(a) shows behaviour of inverter output voltage during switching from stand-alone to grid at 2.5 sec. and Fig. 5(b) represents transition from grid to stand-alone mode at 8 sec. There is no such variation in load d-axis and q-axis voltage as shown in Fig. 5(c), 5(d).

When grid is recovered, combination of filter and grid current flows through load as shown in Fig. 1. So high inrush current as represented in Fig. 6(a). It happened at the instant of 2.5 sec. The frequency is maintained at 50 Hz even during transient as shown in Fig. 6 (b) and within 0.02 sec current peak reduces and remain steady.

For machine side converter, d-axis component of machine current remain constant throughout the operation, as flux remain constant as portrayed in Fig. 8(d). The actual speed of the machine is following the reference speed generated from dc link voltage controller during stand-alone mode as shown in Fig. 8(b). During transition at 2.5 sec (from stand-alone to

grid mode), the dc link voltage increases up to 460 V during transient period and it settles back to 400 V within 0.7 sec. During grid mode, the actual speed is maintained at 79 rad/s and it follow the reference speed provided by the user. So the active power component i.e. q-axis component of the machine current which is generated from the speed controller follows the reference current and verify the flexibility of the controller as shown in Fig.8(c) throughout the operation.

Similarly during switching from grid connected mode to stand-alone at 8 sec, tie line current reduces to zero as portrayed in Fig. 6 (a). During this transition, dc link voltage reduced to 360 volt and take 0.02 sec to settle down. So a big dip is created in load voltage. It is clearly visualized from the d-axis component of load voltage at 8 sec as shown in Fig. 5 (b), (c). Also this changes happen in load phase current as displayed in Fig. 6(d).

During stand-alone mode, voltage controller is implemented for load side converter to compensate the drop of the filter. The d-axis component of the load voltage is maintained at 163 volt throughout the operation as shown in Fig. 5 (c). The harmonics of load voltage and current are 2.79% and 2.02% respectively as shown in Fig. 7(a,b).

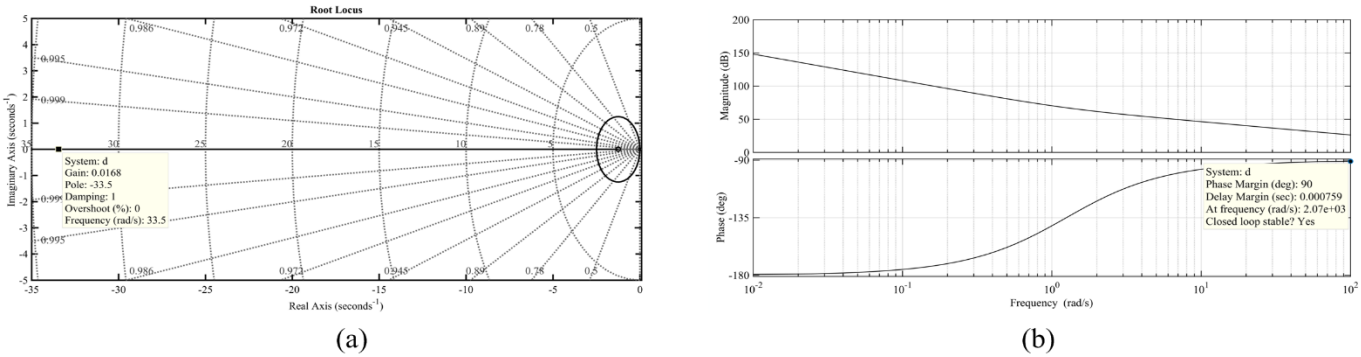

Figure 4. Dc-link voltage controller analysis (a) Root locus (b) Bode plot

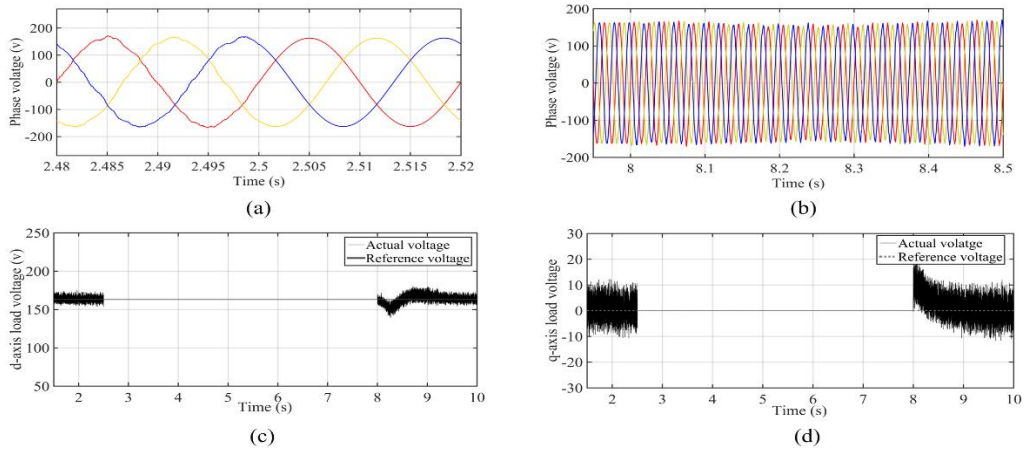

Figure 5. The transient performances of (a) Phase load voltage from stand-alone to grid, (b) Phase load voltage from grid to stand-alone, During transition from stand-alone mode to grid and vice-versa(c) d-axis component of load volatge (d) q-axis component of load voltage

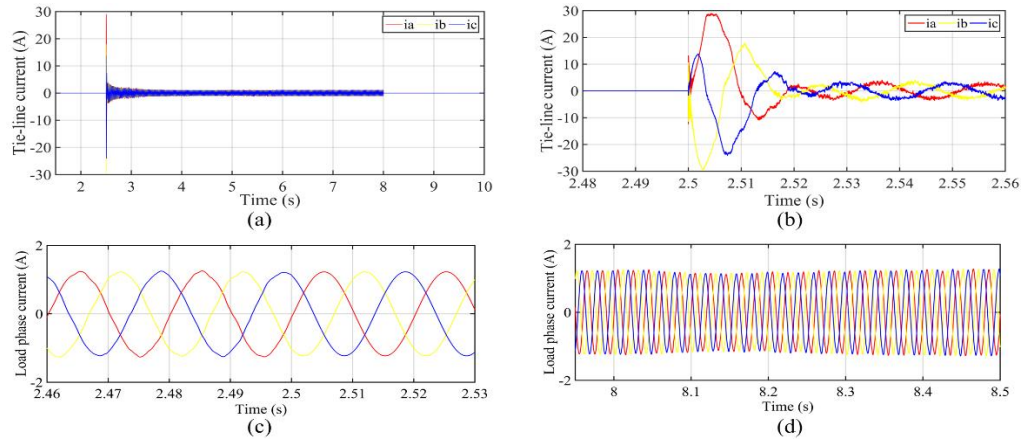

Figure 6. The transient performances of (a) tie line current during transition from stand-alone to grid and vice-versa, (b) zoomed view of tie line current during switching from stand-alone to grid, Phase load current (c) during transition from stand-alone to grid (d) during switching from grid to stand-alone mode

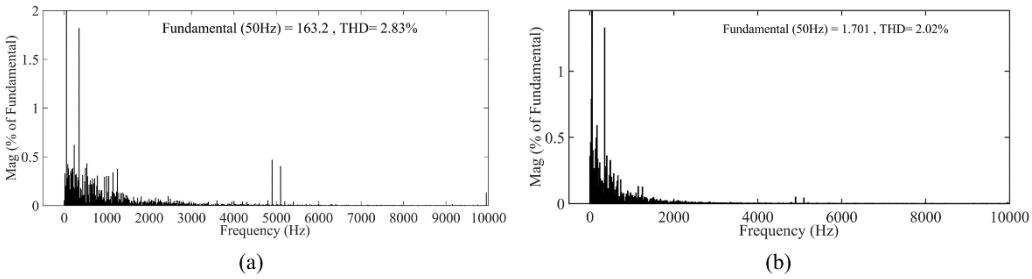

Figure 7. FFT analysis during stand-alone mode (a) load voltage (b) load current

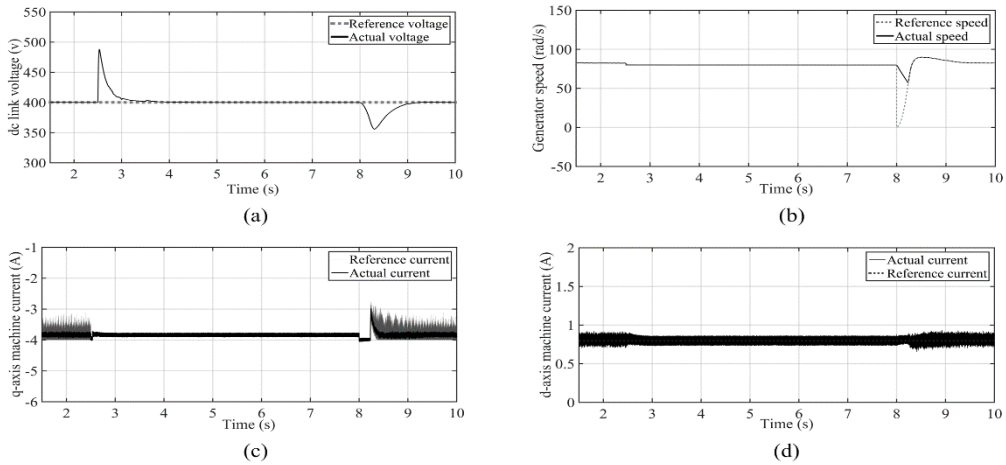

Figure 8. The transient performances of machine side variable during transition from stand-alone mode to grid and vice-versa (a) dc-link voltage (b) generator speed (c) q-axis component of machine current (d) d-axis component of machine current

6. CONCLUSION

The implementation of the flexible control of SCIG, fed by constant prime mover, to operate in grid-tied or stand-alone modes of operations is discussed. The generator speed is changing to extract the power from the input in such a level, that the dc-link voltage is maintained throughout the stand alone mode of operation. During stand-alone mode, the load side converter is regulated to compensate the voltage drop of the filter. The maximum THD for load voltage is 2.83% and for current is 2.02%. Keeping the filter output voltage same as the grid voltage in stand-alone mode of operation allows the transition of all the controllers to grid-connected mode successfully. The tie-line current variation is settled within 0.02 sec during switching from stand-alone mode to grid-tied mode. However the variation is almost not there during switching from grid-ties mode to stand-alone mode. All other variables are found to track their references successfully throughout the transition of the controls. The controller operation during grid-mode is making the system reliable for wind-energy system.

REFERENCES

[1] Chen Z, Guerrero JM, Blaabjerg F. (2009). A review of the state of the art of power electronics for wind turbines. IEEE Trans. Power Electron 24(8): 1859–1875.

[2] Tapia G, SantamarÍa G, Telleria M, Susperregui A. (2009). Methodology for smooth connection of doubly fed induction generators to the grid. IEEE Transactions Energy Conversion 24(4): 959-971.

[3] Blaabjerg F, Chen Z, Kjaer SB. (2004). Power electronics as efficient interface in dispersed power generation systems. IEEE Transactions on Power Electronics 19(5): 1184-1194.

[4] Pena R, Cardenas R, Blasco R, Asher G, Clare J. (2001). A cage inductiongenerator using back-to-back PWM converters for variable speed grid connected wind energy system. Proc. IECON Conf. (2): 1376–1381.

[5] Hazra S, Sensarma P. (2011). Vector approach for self-excitation and control of induction machine in stand-alone wind power generation. IET Renewable Power Generation 5(5): 397-405.

[6] Yang L, Xu Z, Ostergaard J, Dong ZY, Wong KP. (2012). Advanced control strategy of DFIG wind turbines for power system fault ride through. IEEE Transactions on Power Systems 27(2): 713-722.

[7] Zandzadeh MJ, Vahedi A, Zohoori A. (2012). A novel direct power control strategy for integrated DFIG active filter system. 20th Iranian Conference on Electrical Engineering (ICEE2012), Tehran, pp. 564-568.

[8] Ghosh S, Kamalasadan S. (2016). An energy function-based optimal control strategy for output stabilization of integrated DFIG-flywheel energy storage system. IEEE Transactions on Smart Grid (99): 1-10.

[9] Pattnaik M, Kastha D. (2010). Control of double output induction machine based stand alone variable speed constant frequency generator with nonlinear and unbalanced loads. IEEE PES General Meeting, Minneapolis, pp. 1-8.

[10] Combes P, Jebai AK. (2018). Modeling and analyzing the stability of an induction motor drive system using an output LC filter. PCIM Europe 2018; International

Exhibition and Conference for Power Electronics, Intelligent Motion, Renewable Energy and Energy Management, Nuremberg, Germany, pp. 1-8.
[11] Balaguer IJ, Lei Q, Yang S, Supatti U, Peng FZ. (2011). Control for grid-connected and intentional islanding operations of distributed power generation. IEEE Trans. Ind. Electron. 58(1): 147–157.
[12] Bose R, James J. (2014). Control schemes for intentional islanding operation of distributed generation. 2014 International Conference on Power Signals Control and Computations (EPSCICON), Thrissur, pp. 1-6.
[13] Teodorescu R, Blaabjerg F. (2004). Flexible control of small wind turbines with grid failure detection operating in stand-alone and grid-connected mode. IEEE Trans. Power Electron 19(5): 1323–1332.
[14] Kulkarni OV, Doolla S, Fernandes BG. (2017). Mode transition control strategy for multiple inverter-based distributed generators operating in grid-connected and standalone mode. IEEE Transactions on Industry Applications 53(6): 5927-5939.
[15] Mahmood H, Jiang J. (2014). A control strategy of a distributed generation unit for seamless transfer between grid connected and islanded modes. 2014 IEEE 23rd International Symposium on Industrial Electronics (ISIE), Istanbul, pp. 2518-2523.
[16] Arafat MN, Palle S, Sozer Y, Husain I. (2012). Transition control strategy between standalone and grid-connected operations voltage-source inverters. IEEE Transactions on Industry Applications 48(5): 1516-1525.
[17] Mishra R, Saha TK. (2016). Development of a standalone VSCF generation scheme through three stage control of SCIG. 2016 IEEE Region 10 Conference (TENCON), Singapore, 2016, pp. 3538-3541.